3

Antennas and antenna diversity

Patrick C.F. Eggers, CPK, Denmark

The antennas are the outermost components in the transmission chain which are deterministically describable and physically manufacturable. However the network performance of the antennas is not dependant on the antenna alone, but on the interaction between antenna and radio environment. This causing the network performance evaluation of the antenna system to be of a stochastic nature. The primary task for the antenna is

- connection

that is seeing to that any information is conveyed from transmitter to receiver. Equally import are the possibilities to include the antenna to

- suppress or repair media impairments

There are three major areas that have been considered when using antennas for compensating for the impairments of the mobile radio channel:

- noise suppression through antenna gain and effectivity
- temporal fading and interference suppression through multiport antenna diversity
- spatially selective interference suppression through adaptive antenna directivity

The following sections discuss the design and application of antenna elements and systems to meet these tasks. The first section 3.1 covers physical and electrical design of antenna elements mainly used for propagation experiments. Section 3.2 covers the interaction between base station antennas and the radio environment, which influence the perceived antenna diagram. Design criteria for antennas for handportables and influences on human body absorption, are discussed in section 3.3. This both through efficiency and absorption by the human head. The remainder sections 3.4 to 3.6 focus on three key areas in antenna diversity. That is the antenna system structure, the use of an antenna system via combiners and lastly the expected gain in terms of radio channel parameters.

3.1 Antenna design

Ernst Zollinger, IMST, Germany

3.1.1 Extremely wideband antennas

Design of a wideband conical monopole antenna

Fig.3.1 depicts the cross-section of an extremely wideband conical monopole antenna that was developed for radio channels measurements

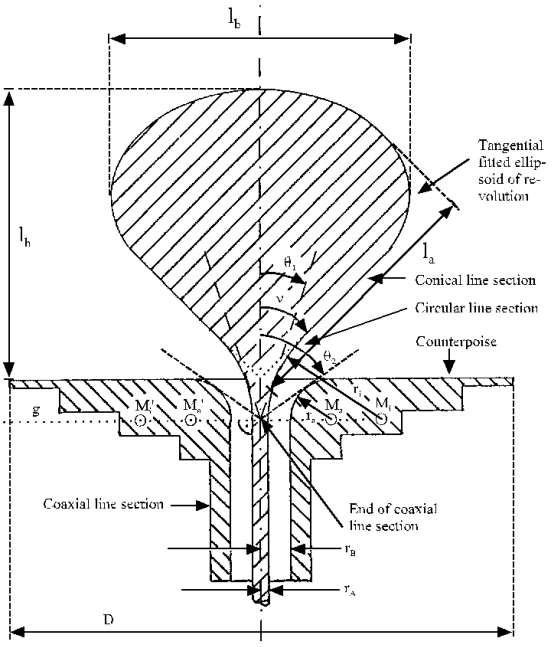

Fig.3.1 Cross-section of a conical monopole antenna

[1]. The feeding point impedance Z_{CO} of the monopole antenna can be matched to the intrinsic impedance Z_{CA} of the feeding coaxial cable by choosing angle ν accordingly.

$$Z_{CO} = \left(Z_0 / 2\pi\sqrt{\varepsilon_r'}\right)\ln\left(\cot(\nu/2)\right)$$

$$Z_{CA} = \left(Z_0 / 2\pi\sqrt{\varepsilon_r'}\right)\ln\left(r_B / r_A\right)$$

Z_0 denotes the intrinsic impedance of free space, r_A and r_B are the radii of the inner and outer conductor of the feeding cable, respectively, and ε'_r is the real part of the complex relative permittivity of the dielectric between the two conductors.

This antenna behaves like an inhomogeneous, open line at low frequencies. Therefore, it is hardly possible to ensure the required performance below a frequency f_L for which the length l_a of the conical section become smaller than approximately $l_a = c/(4f_L) = \lambda_L/4$ where c denotes the vacuum speed of light and λ_L the wavelength. For f_L = 600 MHz the length l_a has to be >12.5 cm. According to [2], the shape of the upper part of the conical antenna section has a strong influence in achieving good performance of the antenna at the lower cut-off frequency f_L. In agreement with [2] and [3], experiments showed that a strongly rounded upper part of this section will substantially decrease the SWR at the feeding point of the antenna at f_L. An ellipsoid of revolution, a hemisphere, a cylindrical superstructure or a combination of the above is well suited for this purpose.

According to these shapes different length-to-diameter ratios l_h/l_b are obtained. In agreement with [2] widest bandwidth was obtained with a length-to-diameter ratio in the range of 0.9 to 1.1. The transition zone between the coaxial line and the conical structure of the antenna is important in achieving a low reflection coefficient at high frequencies. The theory for this problem is well known and can be found in [2] and [3]. The solution is a circular line which is obtained by stringing together conical lines with continuously increasing aperture angles while keeping the intrinsic impedance Z_{CI} constant. For a reflection free transition between the coaxial and the circular line as well as between the circular and the conical line, the corresponding intrinsic impedances must coincide, i.e. $Z_{CA} = Z_{CI}$ and $Z_{CI} = Z_{CO}$. To fulfil the first equation, the centres M_i and M_a of the curvature of the circular line must be on the plane that is perpendicular to the symmetry axis of the antenna. This plane is indicated in Fig.3.1 by the dotted line g. The corresponding radii r_i and r_a are given by $r_i = r_a(r_B/r_A) + (r^2_B - r^2_A)/2r_A$. The diameter D of the counterpoise affects the electromagnetic field in the near- and far-field zone of the antenna, the impedance Z_{CO}, the reflection coefficient and the SWR at the feeding point. Because the transfer function of this antenna has a high-pass characteristic, the SWR increases sharply at the lower cut-off frequency f_L = 600 MHz (Fig. 3.4 and Fig. 3.5). Based on the results outlined in [4] for thin λ/4-monopole, D/λ_L should be ≈ 0.9 for a SWR < 1.25 and ≈ 0.4 for a SWR < 1.5. Therefore, D = 0.426 m and D = 0.259 m have been selected for antenna no. 1 and 2, respectively.

Properties of the wideband conical monopole antenna.

Two wideband monopole antennas have been built (Fig. 3.2 and Fig. 3.3) [1].

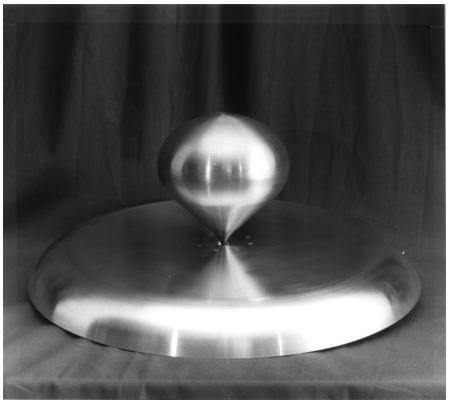

Fig. 3.2 Monopole antenna no. 1.

Fig. 3.3 Monopole antenna no. 2.

Their SWR are shown in Fig. 3.4 and Fig. 3.5 for frequencies between DC and 5 GHz. Extremely wideband measurements showed that the bandwidths of antenna 1 and 2 are 15 GHz and 8 GHz, respectively, if SWR < 1.9 is the criterion.
The co-polarisation patterns of the two antennas have been measured at 1.5 GHz (Fig. 3.6 and Fig. 3.7). For vertical polarisation of the measured antenna θ_A denotes the angle with respect to the vertical axis.

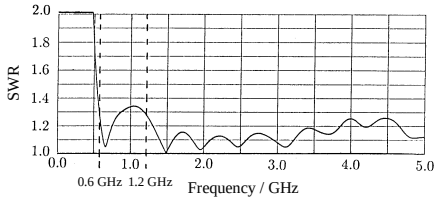

Fig. 3.4 SWR of monopole no. 1.

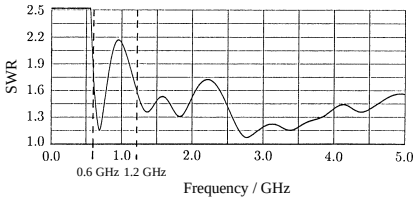

Fig. 3.5 SWR of monopole no. 2.

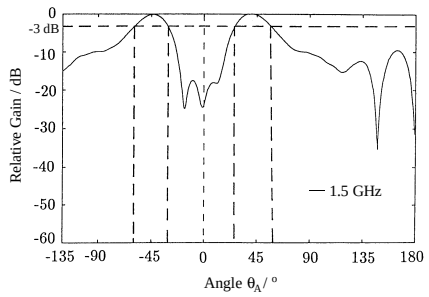

Fig. 3.6 Co-polarisation pattern of monopole antenna no. 1.

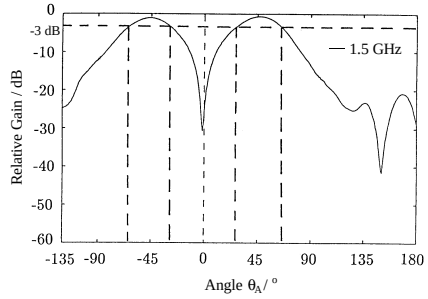

Fig. 3.7 Co-polarisation pattern of the monopole antenna no. 2.

3.1.2 Millimetre-wave antennas

General Considerations

In mobile systems, small size, low power consumption, conservative exposure limits of less than 1 mW/cm^2 [5][1] and low prices are essential requirements. At millimetre-

[1] Currently everything indicates that the limits to be standardised will be adopted from the IRPA/INIRC (International Non-Ionizing Radiation Commitee of the International Radiation Protection Association) „Interim guidelines on limits of exposure to RF fields“ [5]. According to a statement of the IRPA these limits are based on a summary and an assessment of scientific works that have been published by the UNEP/WHO (United Nations Environment Program / World Health Organisation) in the „Environmental Health Criteria“ series.

(mm)-waves, where the link budget is a critical issue, antennas with more than 10 dB gain providing uniform cell coverage are needed.

Patch antennas

Patch antennas printed on top of a PCMCIA card, which protrudes a few centimetres outside of the computer case are suited for ad hoc radio LAN systems where portable computers communicate peer-to-peer. To obtain circular symmetrical radiation patterns with a null at zenith, and maximum radiation in the plane of the PCMCIA card, a circular patch antennas operated in the TM_{02} mode has been designed and tested ([6], [7], [8]). At the operation frequency, a patch antenna can be viewed as a resonator. Following [9], the resonant frequency f_r of the TM_{02} mode circular patch antenna is given by $f_r = f_0/\sqrt{(1+D)}$, $f_0 = 3.832/2\pi\sqrt{(\mu_0\varepsilon_1)}$, $\Delta = (2d\varepsilon_0/\pi\varepsilon_1 a)[\ln(\pi a/2d) + 1.7726]$, the permittivity $\varepsilon_1 = \varepsilon_0\varepsilon_{r1}$ of the dielectric with ε_0 the permittivity of the vacuum, the radius a of the patch and the substrate thickness d. The modification factor Δ represents the contribution of the stray field at the antenna edge. For the prototype, a substrate with a relative permittivity of 2.55 and d = 3 mm was used resulting in a = 2.05 cm. A SWR ≤ 2.0 has been obtained within a frequency range of 5.1 GHz to 5.42 GHz. The radiation patterns are depicted in Fig. 3.8 for different plane-cuts where $\phi = 0$ represents the plane passing through the feed point.

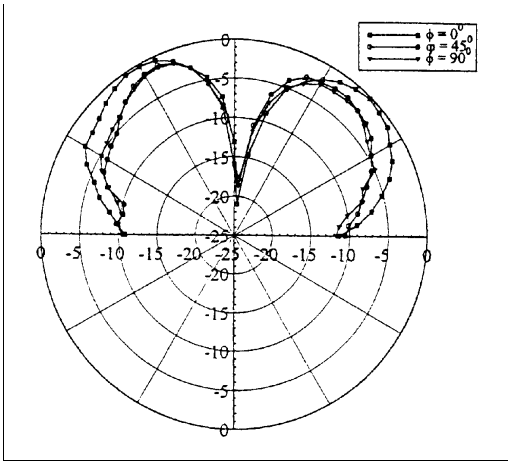

Fig. 3.8 Radiation pattern of the circular patch antenna.

Waveguide antennas

Near uniform cell coverage may be achieved with a conical horn antenna (Fig. 3.9) [10]. It consists of a radial line with spacing a = 2.0 mm and diameter b, a circular waveguide with an interior diameter of d = 3.5 mm, a biconical horn of length L, and an aperture of

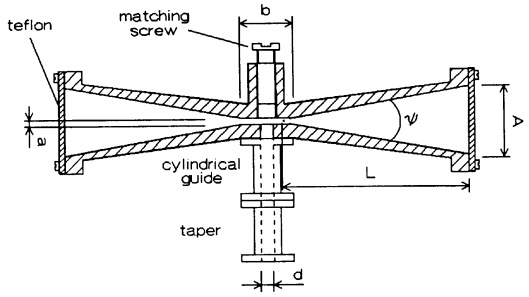

Fig. 3.9 Geometry of biconical horn antenna.

width *A*. An omnidirectional radiation pattern in the azimuthal plane is obtained if the radial line is excited with a circularly polarised TE_{11} mode in the circular waveguide.

The polarisation is horizontal for $\lambda/2 < a < \lambda$ and vertical for $a < \lambda/2$ where λ denotes the free space wavelength [11]. The radiation pattern in the elevation plane is determined by the parameters *L* and *A*. Provided that the differences of the phases in the aperture are smaller then 90°, the magnitude of the electric field pattern can be calculated by the methods described for sectored horns excited with the TE_{01} mode [12]. Excellent agreement between theoretical and measured results have been obtained for the radiation pattern depicted in Fig. 3.10.

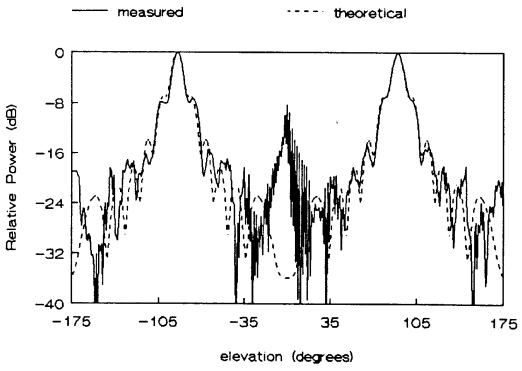

Fig. 3.10 Measured and theoretical radiation pattern in the elevation plane [10].

Dielectric antennas

Dielectric antennas are suitable for mm-wave applications because they are structurally simple and easy to fabricate. Two types of dielectric leaky-wave antennas are of particular interest: tapered dielectric-rod and periodic dielectric antennas. The first is a surface wave antenna radiating in the forward direction. Periodic dielectric antennas consist of a leaky-wave guide created either with a periodic surface perturbation or by generating a leaking propagation mode in the structure.

Both structures can be designed to radiate almost to broadside, i.e. orthogonal to the antenna axis. The most important design parameters are the leakage coefficient α which describes the radiated power per unit length and the phase coefficient β which is determined by the overall effective permittivity ε_{eff} of the dielectric antenna. Both parameters strongly depend on the height of the dielectric but only slightly on the thickness of the periodic surface perturbation.

Compared to microstrip travelling mode antennas, the beam pointing angle of dielectric antennas is strongly frequency-dependent: up to 40^o per 10% variation of the frequency. This feature could be used in a WLAN FDMA/SCPC concept using DCA for a mobile unit in a given azimuth direction of the antenna beam. More information on both types of dielectric antennas can be found in [13].

Dielectric lens antennas directly fed by the waveguide are compact in size, easily assembled and therefore appropriate for mass production. Depending on the shape of the lens near uniform cell coverage can be obtained [14], [15], [16].

3.1.3 Internal antennas for hand sets

Internal antennas are applied in a growing number of mobile communication systems due to design advantages, serviceability and price ([17], [18]). The new radiation-coupled dual-L antenna presented in [19], [20] offers at least 50% higher bandwidth compared to an inverted-F antenna of equal height H (Fig. 3.11) [21]. Its resonant wavelength λ_0 is determined by the geometrical parameters L and H: $L + H = \lambda/4$. The dimensions of the antenna have been optimised using the 333 segment wire-grid model of the program NEC in conjunction with the program AutoCAD. [2]

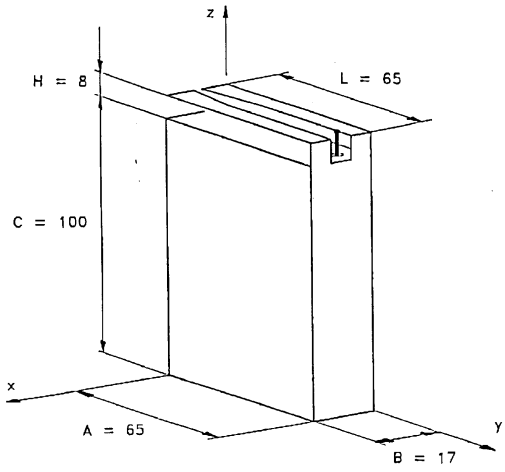

Fig. 3.11 Radiation-coupled dual-L antenna mounted on top of the shielding case of a cordless telephone [19], [20].

The radiation patterns of the antenna have been measured with a test transmitter powered by the original battery pack of the cordless telephone inside the shielding case, which in turn was put into a plastic case. For the wire-grid model the radiation patterns were calculated. Since NEC did not allow to model the influence of the plastic case, the patterns were calculated for frequencies that corresponded to 914 MHz and 954 MHz when the plastic case was absent, i.e. at 970 MHz and 1010 MHz. Particularly for the dominating polarisation the calculated radiation patterns compare well with the measurements.

[2] Registrated trademark of Autodesk, Inc.

3.2 Base station antenna relations

Patrick C.F. Eggers, CPK, Denmark

In the current cellular systems the base station (BS) antennas are mainly mast-mounted omni directional or sector antennas with respect to the azimuthal plane. The use of collinear arrays lead to increased gain by reducing the elevation beamwidth. Beam tilting and shaping of the elevation pattern are used to attempt control of cell contours. Adaptive antenna arrays have been suggested to suppress interference via spatial filtering in an SDMA scheme. The effectiveness of such antenna arrangements are closely linked with the directional properties of the radio environment as sensed at the BS site. Models exist for the angular BS environments with respect to spatial fading [22],[23],[24]. But only little work [25] has been presented, dealing with basic angular domain fading and antenna relations. The following subsections will expand on the radio propagation description in the previous chapter, to include the directional information at the BS and its influence on perceived antenna characteristics.

3.2.1 Angular relations between BS-antennas and radio environments

Basically 2D circular relations in either azimuth or elevation are sufficient for most outdoor small and macro cell applications. In the following we consider small scale relations (mobile station (MS) movements over a few wave lengths (λ)) between antenna diagram 'a' and the environment diagram 'e'. Thus the environment diagram can be considered stationary.

2D circular antenna environment relations

When rotating a BS antenna with directional amplitude radiation pattern $a(\varphi)$ in a circle around azimuth, the measured complex voltage response $m(\varphi)$ is [26]

$$m(\varphi, d) = \oint_{\phi} e(\phi, d) \cdot a(\phi - \varphi) d\phi = R_{e,a^*}(\varphi, d) \qquad (3.1)$$

which can be expressed as a correlation R between the antenna amplitude response and the angular environment diagram $e(\varphi)$. The MS movement is represented in a displacement variable d. The angular frequency relation $\tilde{m}(\omega_\varphi,\omega_d) = \tilde{e}(\omega_\varphi,\omega_d)\cdot\tilde{a}^*(-\omega_\varphi)$, follows from the correlation theorem. Assuming uncorrelated scattering (US) identical relations hold for the mean power diagrams $M=<|m|^2>$ [27]. It follows that standard frequency domain (inverse Wiener) filtering techniques can be used to suppress the measurement antenna's influence on the measured responses [27], [28], yielding an estimated environment response $\tilde{E}'(\omega_\varphi) = \tilde{M}(\omega_\varphi)\cdot\tilde{F}(\omega_\varphi)$. The application of this technique to angular pattern processing was introduced by the RACE II project TSUNAMI [28], [27], using an enhanced inverse filter $\tilde{F}(\omega_\varphi) = \tilde{W}(\omega_\varphi)\cdot\tilde{A}^*(\omega_\varphi) / (|\tilde{A}(\omega_\varphi)|^2 + \alpha\cdot NRS(\omega_\varphi))$. $NSR(\omega_\varphi) = \tilde{N}(\omega_\varphi)/\tilde{E}(\omega_\varphi)$ is the noise to signal ratio, $\tilde{W}(\omega_\varphi)$ is a reshaping window and α is a scalar < 1, chosen to under estimate the noise [29]

Angular correlations

The angular autocorrelation properties are of interest as they represent angle diversity correlation properties, leaning themselves to adaptive beam operations like for example jitter diversity [30]. We have [26]

$$S_{m12}(\omega_\varphi) = \tilde{m}_1(\omega_\varphi) \cdot \tilde{m}_2^*(\omega_\varphi) = S_{e12}(\omega_\varphi) \cdot S_{a12}^*(-\omega_\varphi) \qquad (3.2)$$

Also from the correlation theorem we have

$$R_{m12}(\varphi) = \oint_\phi m_1(\phi) \cdot m_2^*(\phi - \varphi) d\phi = F^{-1}\left[S_{m12}(\omega_\varphi)\right] = R_{e12}(\varphi) \otimes R_{a12}^*(\varphi) \quad (3.3)$$

Thus the angular correlation function is described by a convolution between the individual correlation functions of the environment and antenna [26]. This correlation expression is general with respect to orientation angle and This correlation is different from those derived for the temporal or spatial fading responses caused by a moving MS [31]. Those type of correlations are orientation specific and thus relevant to the fixed beam operations discussed in section 3.4 to 3.6. Wide sense stationarity (WSS) has been assumed for the previously mentioned angular correlations. Note that this may be more difficult to satisfy for angular than for spatial fading, in particular if the environment is very selective, i.e. it has a narrow beamwidth distribution.

Angular diversity coherence measures.

The complex auto correlation coefficient function is $\rho(\bullet)=R(\bullet)/R(0)$, due to the previous US assumption. In case of pure angle diversity we can define an angular coherence beamwidth $ABW_{0.7} = \varphi\big|_{|\rho(\varphi)|^2=0.7}$ [26]. This beamwidth is the coherence measure of the angular fading experienced by a BS antenna sweeping in the angular domain. It is also possible to define pattern and space coherence measures for the angular fading [26].

Quantitative angular spreading parameters

First and second order moments of the mean power response have been proposed [26] for a statistical description of the small scale angular environment mean direction and spreading. An angle of a defined Centre of gravity can be used as an unambiguous estimate of the mean angle [27].

A transform of the angular mean power pattern from a circular to a linear representation (power angular profile PAP [26]), provides analogy to the power delay profile (PDP) in the temporal domain. Similar dispersion parameter definitions can be applied to the PAP, as those commonly used for the PDP [32]. The angular spread S_φ follows from [33] as the standard deviation of the PAP, analogue to the delay spread on the PDP. Similar to the delay spread properties, variance subtraction can be used

to suppress the influence of the antenna on the measurement $S_{E_\varphi}^2 = S_{M_\varphi}^2 - S_{A_\varphi}^2$ [26]. The only difference compared to the delay spread case, comes in a sign change concerning the mean angle relation, $\overline{\varphi}_E = \overline{\varphi}_M + \overline{\varphi}_A$. A requirement to apply these properties to the PAP, is that the environment pattern is well confined around the mean angle.

A parameter reflecting the large scale angular spreading of the environment is the effective sidelobe level [27].

Antenna gain

The effective BS antenna gain saturates when increasing the directivity [30]. Namely when the antenna becomes more selective than the environment. Then the increased directivity is counter-balanced by less received environment power, due to spatial filtering.

3.2.2 Environmental influence on perceived antenna pattern

Pattern distortions by nearfield disturbances

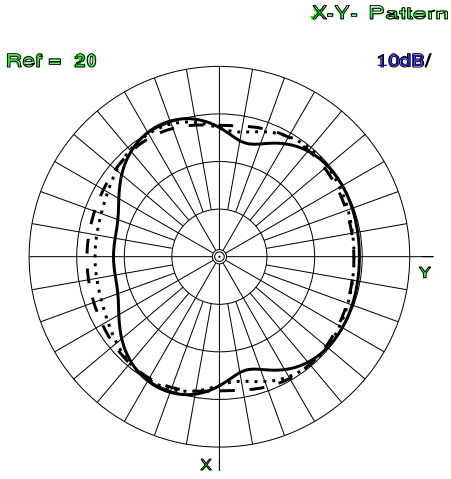

Fig. 3.12 Pattern influence of a mast placed 30 cm behind 8-element collinear array [34]. Mast diameter very small (dashed), 5cm (dotted) and 10 cm (solid).

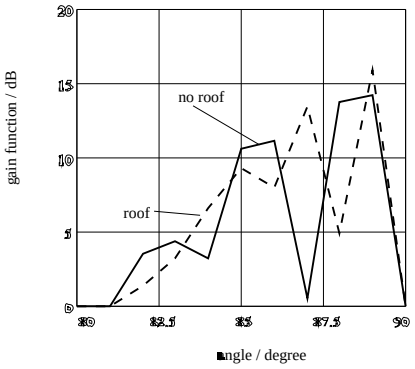

Fig. 3.13 Elevation pattern influence of roof 3m below antenna (detail near the main lobe) [34]. Roof (dashed) and no roof (solid).

Antenna mountings and other objects in the near field cause pattern distortions. This becomes particularly important where cell splitting is extensively used to gain capacity. Small-cell antenna systems are often placed on roof tops without the clearance found at mast mount macro cell sites.

Using the method of moments (MoM) [34] has performed simulations of an 900 MHz collinear array BS antenna subject to nearfield disturbances. The findings are that the azimuthal pattern is distorted less than 2 dB if the antenna mast distance is 1m for a 10 cm thick mast. For a spacing of 30 cm the mast influence is noticeable as seen in Fig. 3.12. Pattern distortion of the mounting rods are found negligible. For a typical small cell antenna at 30 m height above ground, there can be around 10 dB pattern difference whether placed on a 27 m roof or on a free standing mast. This is particularly the case for the main beam area which is also the most critical in determining cell boundaries, see Fig. 3.13. The building influence is indifferent to the exact material parameters, (difference < 3dB):

However the effect found on the BS antennas, stresses the importance of not uncritically applying free space patterns to network planning tools, especially for small cell applications.

Experimental description of sharp gradient pattern shaped antennas

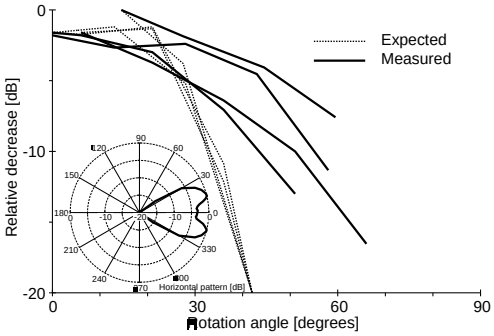

Fig. 3.14 Expected and measured relative angular level decrease for azimuthal shaped antenna pattern [36].

Beam tilting and shaping can be used to enhance cell border definition. Free space properties of a sharp gradient shaped elevation pattern antenna, have proven efficient in small cell urban environments [31]. Shaping of sharp azimuth gradients at the cell edges should ideally provide a more even illumination of a sector and decrease spillover between sectors [35], [36]. However in the azimuthal case the free space shaping is not reflected in an similarly perceived pattern in a small-cell urban environment [36] (900 MHz measurements rotating the shaped antenna in 15^{o} steps,), see Fig. 3.14.

From the previous subsection, we have that the perceived pattern is a correlation between antenna and environment. Thus it seems that the azimuthal environment spreading is so wide that the shaping details are 'blurred' by the environment, whereas the spreading in elevation is so compact that the effect of the elevation shaped antenna is still noticeable. This can be explained with the relative low angle of incidence in the elevation plane, where any scattering area around the MS will be perceived strongly compressed in elevation, whereas the azimuthal extension is more dependant on the MS to BS range.

Experimental description of narrow beamwidth antennas

Directional BS experiments at 1.8 GHz have been reported by [27],[28], performed under TSUNAMI. A dual branch wideband sounder has been used together with a 1.9 m dual polarised patch array at the BS. Test where performed with range lengths up 2.5 km. One test used a fixed MS and a rotating BS beam. In this case the small scale angular antenna response was recorded (see Fig. 3.15.) It is seen how the received energy is scattered both in delay and angle and thus makes it difficult to associate a main beam direction between MS and BS.

Main conclusion of these tests are, that when comparing main beam responses of highly directional antennas to omnidirectional antennas:

- Delay spread reduction about a factor two or more
- Increase in polarisation purity (XPD) by a few dB

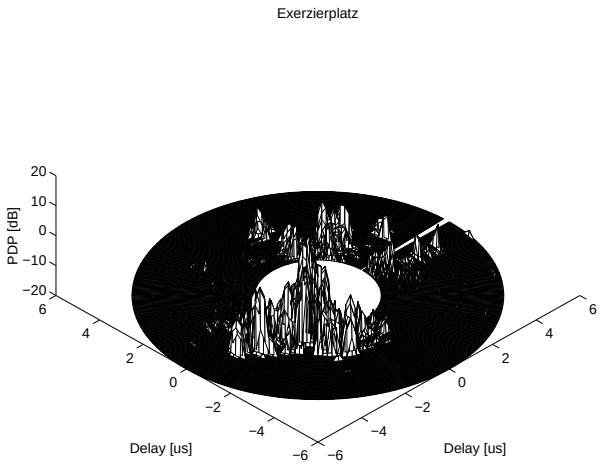

Fig. 3.15 Angular scattering function at a BS, .i.e. PDP versus angle.

The absolute environment XPD figures (around 6dB urban and 12dB rural) sets limits to the worthwhile XPD to target in design of dual polarisation antenna systems.

A second test used a fixed BS beam and a MS driving through boresight, thus revealing the large scale perceived BS antenna pattern. The most important information gained form this test is the distortion of the free space antenna pattern (correlation with the environment spreading function), which results in

- Reduction of perceived antenna sidelobe suppression to about 10 dB in urban small cell environments, (20 dB in open rural areas)

These findings are also supported by urban microcell measurements on a DECT testbed by [37] and shown in Fig. 3.16. The shoulders of the measured antenna response are about -10 dB whereas the free space pattern (solid line) drops below -15 dB when over 90° from boresight. This degradation in effective sidelobe level has importance for SDMA capacity calculations as the environments set a limit to the spatial interference suppression one can expect from an antenna in a traditional beam oriented operation. On the other hand the same limit eases sidelobe suppression requirements of the antenna beam design itself. Bettering the free space sidelobe suppression below that supported by the environment, will not give any return in terms of gain in system performance.

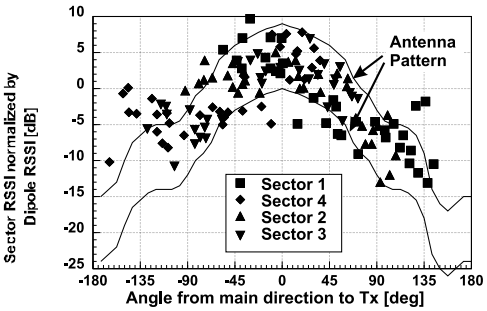

Fig. 3.16 Measured RSSI for sector antennas normalised by measured RSSI for omni directional dipoles [37].

3.2.3 Adaptive base station antenna arrays

Hardware adaptive antenna testbeds

A real-time hardware adaptive antenna testbed, based on a DECT radio interface and digital baseband beamforming, is developed by TSUNAMI [38]. The antenna array consists of 8 dual polarised wideband patch antennas[39].

Algorithms

The algorithms used in the TSUNAMI tests can be grouped into:

- Beam oriented (SDMA, grid of beams, beam jitter)
- Signal combination (selection, maximum ratio etc. diversity)

The first group deals with beam approaches and leans it self to spatial tracking of a MS and possible providing nulls in directions of interferers. These techniques can be applied both on up- and down-link as they mostly rely on mean direction to the MS which is fairly slowly varying. Contrary, the signal combinations approaches which rely on complex weights optimisation on small scale channel variations (optimum combining etc.), only seem feasible in up-link applications, even in TDD systems [40].

The TSUNAMI testbed provided early demonstrations of real-time SDMA-like operation (two users supported, that occupy same frequency and time slot) using MUSIC in LOS environments (note that in time dispersive environments this algorithm will have strong difficulties) [41].

Furthermore the testbed also showed real-time functionality of newer type antenna diversity, namely angular domain jitter diversity [30],[42].

Using 3D UTD simulation of indoor propagation environments (7m x 200m x 160m total) [43], the angular distribution and dependence of PDP's is predicted. This used in a 10-20Mb/s 1.8 GHz adaptive antenna system simulation, using a circular array and direct matrix inversion (DMI) as adaptation scheme. Conclusion are that 8 elements are needed to bring BER's below 10^{-3} and that BER's rise to about 10^{-2} when decreasing array diameters from 2 to 0.5λ
High resolution algorithms like 2D ESPRIT can estimate azimuth and elevation concurrently [44]. In a strongly elevation dispersive environment (as for example indoors), failing to estimate elevation can cause errors up to 40^{o} in the azimuthal estimate [44]. This will though hardly be a problem for outdoor macro cell base station situations.

For beam oriented approaches, a few guidelines can be set when designing the antenna aperture

- Size: for beam jittering, so possible 3 dB array beamwidth is less than minimum expected 3 dB beamwidth of the environment [30]. For beam griding or SDMA operation, the array beamwidth can be much larger, depending on the number of users to support within a sector.
- Number of elements: enough when a sidelobe level suppression better than about 20 dB (open rural terrain) or about 10 dB (urban environment) can be reached [28].

For signal combination approaches, the requirement on element spacing is port decorrelation (see section 3.6) and the number of elements depends on the number of interferers to suppress [40].

3.3 Antennas for portables

Gert F. Pedersen, CPK, Denmark

Most antennas for portables today are external wire antennas, typically half-wave dipoles but also quarter waves and partly helical types in order to make them smaller and better matched. The half-wave dipole antenna is a good candidate for portables in respect of antenna performance, but there are practical problems with external antennas and most work in COST231 has therefore been on internal antennas.

For the design of integrated antennas there are two main goals. One is to obtain high antenna performance due to the limited power available, the other goal is to reduce the absorption in the human head. These goals are not necessarily mutually exclusive, which has been demonstrated by an antenna design in [45].

3.3.1 Antenna performance

An integrated antenna with high performance is characterised by large bandwidth and low volume. The polarisation of the antenna is also important due to the cross

polarisation arising from different environments. It is preferable if the antenna design is unaffected by a change in the physical dimension of the handset, whereby reuse of the antenna is possible.

To fulfil this the current must be concentrated near the antenna and not distributed throughout the entire handset. Also the physical location of the antenna is important. If it is placed very near to parts of the human body high losses will result. A quarter wave monopole on top of the handset will give large antenna currents distributed all over the handset, because the handset and antenna act as an asymmetrical dipole. This results in relative high antenna currents placed just under the plastic cover a few millimetres from the users head/hand, and high losses follows.

In a frequency division duplex system, the bandwidth of an antenna needs only to cover the up and down link band and not the guard band, in order to keep the volume low [45]. The relative bandwidth requirements for GSM/DCS-1800/NMT900 changes from 7.6% to 5.4%. It is important to design a good average match for the handset used in speaking position and in standby, see Fig. 3.17

Low volume to bandwidth ratio is important when considering internal antennas and the Radiation Coupled Dual-L Antenna is a good example of an integrated antenna with high bandwidth to volume ratio [18].

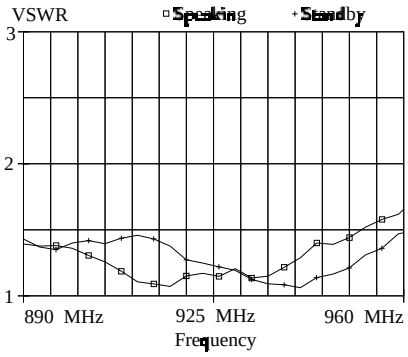

Fig. 3.17 The VSWR as a function of frequency for the FS-PIFA both for the handset used in speaking position and in standby [45].

The performance of an integrated antenna should be found by comparing it to other antennas using the conditions where the antennas are used. Most present handportables for GSM/NMT900 use a half wavelength whip antenna. It is therefore used as reference antenna in measurements of average received power from a BS using the handsets in normal speaking position [45]. These measurements have been carried out in natural user environments. From the field test average received power is calculated and the results are tabulated for three types of environment.

Measurement	Environment	Dipole	FS-PIFA
Average	Indoor	0dB (-85.58dBm)	-1.85dB
received	Around buildings	0dB (-76.10dBm)	-2.2dB
power	Inside moving car	0dB (-69.45dBm)	-2.77dB

Table 3.1 Average received power obtained from measurements. The figures in brackets are average received power in dBm, the other figures are average received power relative to the dipole in dB.

In all measurements, the handset is used as the receiver, and a fixed GSM- channel (BCCH, channel 94 at 953.8MHz) from a BS is used as "transmitter". Although the instantaneous power changes, the average power remains constant, as no power control is employed at the base station for this channel. The results of the gain measurements are shown in Table 3.1.

About 4 million samples were taken. Due to the absorption, losses in the plastic casing (2 mm thick) and shadowing, the integrated antenna has about 2 dB smaller gain than the dipole. The smallest gain difference is inside the buildings. One explanation is the more omnidirectional distribution of effective scatterers inside a building, making the average gain somewhat independent of the radiation pattern and the polarisation

3.3.2 Antenna configurations for reducing body loss

To obtain low absorption, all antenna current should be located as far as possible from the user's head/hand. This means controlling the current so that nearly all current is concentrated very close to/in the antenna, and placing the antenna as far from the users head/hand as possible, i.e. on the back of the handset. The radiation will then be away from the users head and not omnidirectional [46]. An omnidirectional antenna on a handset in normal speaking position, will anyway result in relatively higher radiation directed away from the users head due to losses. The size of the antenna must also be large to get a uniform current distribution over the antenna. Hereby no high current point, as the source point of a dipole, will arise.

Thus the possibility of a high SAR (specific absorption ratio) is avoided even when the handset is used in an abnormal position. Whereas it is rather easy to predict where the user will place the handset relative to the head, it can be difficult to predict where the user will place the hand. The above goal forms the new design criteria together with the fact that the antenna must be quite large but not occupy a large volume [45]. The latter, in order to control the current in a way so that the antenna can radiate by it self and minimise the coupling to the casing.

When the antenna has to be large the possibility that the user grips around or touches the antenna arises. But with careful design of the handset itself, so the user grips naturally elsewhere, this problem can be solved at 900 MHz and as frequency increases it becomes less difficult.

Present standards for handheld antennas are not only concerned about total average absorption, but also about the maximum local SAR averaged over 1g or 10g tissue. The highest SAR value measured for the FS-PIFA when the handset is used in different speaking positions is 0.19 mW/cm^3 averaged over 1g of tissue and 0.12 mW/cm^3 averaged over 10g of tissue. These figures are about 10 times lower than both the ANSI standard (1.67 mW/cm^3 averaged over 1g) and the German standard (2.0 mW/cm^3 averaged over 10g), whereas the same figures for different present-days handportable investigated by [47] all violate the criteria when used in worst case.

The FS-PIFA has demonstrated that it is possible to produce an integrated antenna with a sufficiently good match over the GSM duplex bands. The effective gain is about 2 dB less than a $\lambda/2$ dipole, but the local absorption rate about ten times smaller than required from standards and found in existing portable antennas.

Comparing with earlier results on quarter wave monopoles on handsets [48], it is apparent from Figure 3.18 and 3.19 that the influence of the head is much smaller for

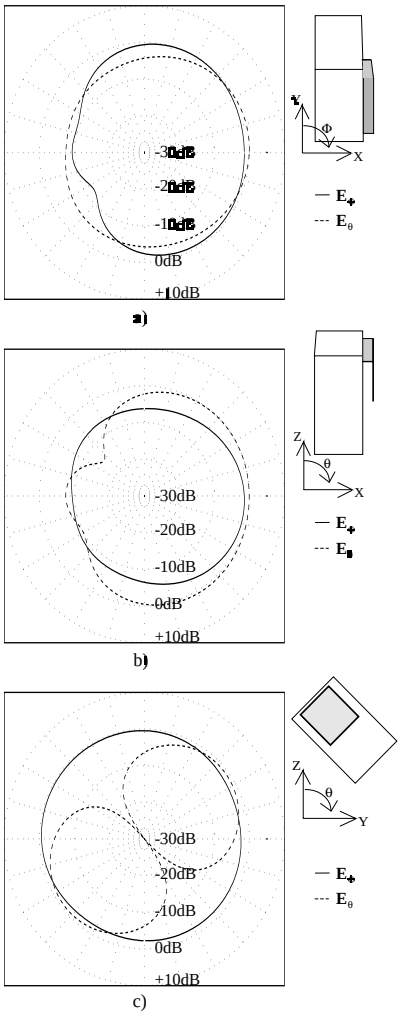

Fig. 3.18 The radiation pattern for the handset *without* a model of the human head and hand. The handset is tilted 45^o, as in ``normal" speaking position a) XY-plane b) XZ-plane c) YZ-plane

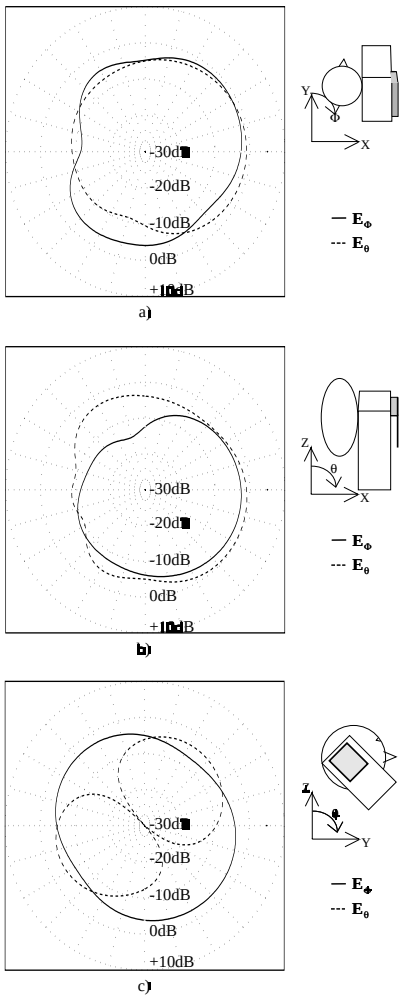

Fig. 3.19 The radiation pattern for the handset *with* a model of the human head and hand. The handset is tilted 45^o, as YZ-in ``normal" speaking position a) XY-plane b) XZ-plane c) plane

the integrated antenna with reduced radiation towards the head. The integrated antenna tends to radiate more upwards and downwards. This may explain some of the relative lower effective gain. However this may be the price to pay for an integrated antenna with low local absorption.

3.4 Mobile and base station diversity techniques

Silvia Ruiz Bouqe, UPC, Spain

The local fluctuation of the signal strength, the fading, caused by propagation along multiple paths and shadowing objects between a base station an a portable unit makes it necessary to have a margin when designing the radio link budget in a system with high reliability.

This margin can be lowered by use of diversity, i.e. transmitting or receiving replicas of the information signal over decorrelated channel conditions. Diversity relies on the principle of repair by use of redundant information (several 'copies' of the information signal) and can thus enhance link quality or allow same quality over poorer channel conditions.

As will be seen later in section 3.5 and 3.6 the effectiveness of a diversity system depends on decorrelation of the diversity branch channel conditions. For most cases the fading envelope of radio signal is used as a measure of channel impairment. Traditionally it thus falls natural to use the envelope correlation coefficient (ρ) between branch output fading signals, as figure of merit for the diversity system. For analogue systems or digital systems employing interleaving, ρ≅0.7 is normally regarded as sufficient for worthwhile deployment of a diversity scheme. This section will focus on the construction of antenna system structures and their ability to decorrelate branch fading signals.

In experiments, care must be taken to assure proper quality of recorded signals on which correlation coefficients are calculated . It can be shown that the envelope correlation coefficients of Rayleigh fading signals subject to additive Gaussian noise, degrades as a second order function of the signal- to noise ratio (SNR) [49]

$$L(SNR) = \frac{\rho_{12,\,fading+noise}}{\rho_{12,\,fading}} = \frac{SNR^2}{SNR^2 + 2 \cdot SNR + 1};\quad SNR = \frac{P(Fading)}{P(Noise)} \tag{3.4}$$

I.e. the SNR must be larger than about 20 dB for the correlation estimate to be within 2% of it's noise free value.

3.4.1 Diversity domains

To achieve replicas of the information channel over decorrelated channel conditions, some discrimination or separation in one or more channel domains is needed. The art of establishing a diversity system lies in the way we can obtain and maybe combine domain separations, that lead to a desired channel state decorrelation.

The mobile radio channel domains which can used for diversity separation purposes are:

- Space (space diversity, displacement of antenna centres)
- Antenna pattern (pattern diversity and field component)
- Antenna orientation angle (angle diversity, orientation angle)
- Polarisation (polarisation diversity)
- Temporal/frequency (delay-tap or frequency diversity)

where the first 4 domains normally are thought of as antenna diversity domains, the latter is normally system specific (i.e. through use of equaliser, interleaving, frequency hopping etc.). However decorrelation through separation in the 'antenna domains' will often also lead to decorrelation in the temporal domain.

Normally the correlation between two polarisations undergone scattering in a mobile channel, is considered virtually zero. The determining factor for a polarisation set-up is the power imbalance expressed in terms of the cross-polarisation-discrimination (XPD).

There are a few further general distinctions to be made regarding antenna diversity, that is:

- MS or BS environment
- up-link or downlink power budget
- Macro or micro scenario

The situation for the base station is different from the mobile case since the angular spread of the incoming waves is much smaller, see section 3.2. This leads to a choice of different possibilities of antenna positioning on the mast, including the use of polarisation diversity. Therefor, while the single branch radio channel link is reciprocal, the application of the combined multi branch radio link is not. Thus an antenna diversity structure will not yield the same performance (branch decorrelation) when placed at the MS or BS end of the link.

The significantly better down-link-budget for a mobile system (2W for MS and 15-20 W in BS for GSM system), makes it most advantageous to reduce the multipath fading margin on up-link by implementing base-station antenna diversity. While most diversity action is associated with short term fading (micro diversity), macroscopic diversity (i.e. having more than one base station within each cell) operates on the local mean shadow fading.

Two branches are often considered as a practical number of branches, as any further number of branches only supply little additional diversity gain.

3.4.2 Base station antenna diversity for outdoor environments.

Space Diversity for urban macrocells

The required spacing at the base station, is different for separation in the horizontal and vertical planes, due to the different angular spreading experienced, see section 3.2.

For **horizontal spacing** the separation depends on the angle between the line joining the antennas and the line joining the base station and the mobile (around 20λ when the angle is 90º and 80λ when the angle is 0º) [50]. Both distances increase with the antenna height and decrease with the presence of local scatterers. If **vertical spacing** is considered the required separation is around 15λ but it depends on the scattering of the area in which the mobile is located [33]. In general lower correlation coefficients can be obtained with horizontal separation than with vertical separation [51].

In [52] two different horizontal separation (0.6 and 1.4 m) have been considered with antennas at the top of buildings (10 m high). When the distance between diversity antennas is 0.6 more than half of the measured points has a correlation coefficient higher than 0.9 obtaining a poor diversity configuration. When the distance increases to 1.4 m the correlation properties improve significantly but there are still several locations with a strong cross correlation.

Angle diversity for microcells

In [53] planar-antennas from Huber&Suhner with a gain of 7.5 dBi and 3 dB beamwidths of 80º and 50º for the horizontal and vertical plane respectively were used. In one site four planar antennas were used to cover an angle of 180º with some overlap of the antenna patterns. In other site two pairs of directional antennas were pointing in opposite directions of the street. Horizontal spacing between antennas was arbitrary chosen to 0.4 m. For comparison both sites were also measured using dipole antennas spaced horizontally by 0.2 m. in a two branch selection diversity scheme.

Large differences in received signal for the four angular antenna sectors (received power level 5 to 15 dB lower than the power in the strongest sector) indicates that a significant improvement in CIR can be achieved by using directional antennas and time dispersion will also be reduced.

Polarisation diversity

There are few studies reported in literature about polarisation diversity. This is due to the difference in mean received power between co-polarised and cross-polarised branches when one polarisation is transmitted (cross-polarisation discrimination XPD). which is traduced in a reduction of the diversity gain. Results shown that the XPD is typically between 6-20 dB and that it is much higher in rural or sub-urban than in urban environments and it is also higher in outdoor than in indoor environ-

ments. Also the XPD increases in LOS and decreases with distance. The envelope correlation coefficient is usually higher than the value obtained when considering space diversity. Having uncorrelated polarisation's, a XPD of 10 dB corresponds to an equal branch power (space diversity) system with a $\rho = 0.7$ [54].

Hand-helds with poor antenna polarisation purity and random orientation, will couple energy between polarisations and thus decrease the XPD. This will even further benefit polarisation diversity applications.

Combined Polarisation & Space diversity in urban small and microcells

In [55] the possibility of using polarisation together with space de-correlation at the base station is tested. Transmitter antenna is a quarter-wavelength monopole mounted on the metal roof of a car. A dual branch receiver with two identical planar array directional antennas with an azimuth and elevation 3 dB beamwidth of 60º were used. The antennas have a gain of 8 dBi and a XPD better than 30 dB. Different antenna highs (3 or 30 m above rooftops) and different antenna configurations (horizontal separation between 10-20 λ, vertical separation, different antenna inclination) were tested. In a previous work of the same authors it was found that for large cells (10-20 km cell radius) and working at 900 MHz the XPD was in the range around 4 dB and 12 dB for urban and suburban areas respectively. For small cells and microcells the urban XPD is between 7-9 dB.

The effectiveness of compact (less than 10 λ antenna separation) antenna configuration for urban small a microcell is shown. All configuration provide envelope cross-correlation about 0.7 or less. The individual space and polarisation effects in a combined system are independent and multiplicative [55]. Thus the combined system correlation coefficient can be expressed as

$$\rho_{combined} = \rho_{space} \cdot \rho_{polarization}(\alpha, \Gamma)$$

$$\rho_{polarization}(\alpha, \Gamma) = \frac{\Gamma + \frac{1}{\Gamma} - 2}{\Gamma + \frac{1}{\Gamma} + \frac{1}{\tan^2(\alpha)} + \tan^2(\alpha)} \tag{3.5}$$

where α is the inclination angle of the antenna element with respect to the copolarisation and Γ is the XPD.

Combination of Space and Temporal diversity for downlink operation

There is still a low-cost possibility of reducing the multipath fading margin on the down-link by transmitting a delayed signal on a second antenna branch (uncorrelated though space diversity) in order to introduce more channel time dispersion and thus reduce the coherence bandwidth (pre-Rake transmitter). The delay is in the order of a few bit periods relative to the first branch [56]. The resulting reduction in fading

margin can be about 3-10 dB on down-link (as the GSM equaliser is better exploited) [56].

3.4.3 Base station diversity for indoor environments

Space diversity can also be used in a radio system to reduce the impact of sever fading within buildings. A path separation of few wavelengths is referred to as microscopic diversity (MIC), while a separation equivalent to the distance between the bases in a normal cellular configuration is called macroscopic diversity (MAC). When the separation is between 1 and 10 m intended to be used at one base station is called medium diversity (MED). Of course the system complexity is much lower with the MIC and MED schemes, since the selections can be made at each base station.

Microscopic space diversity

In [57] a space diversity technique is implemented with two quarter-wavelength monopole antennas separated a distance between 0.25λ and 3.5λ and a selection technique. Many measures in LOS and NLOS at 1.6 GHz were done showing that the signal at both antennas is uncorrelated (the correlation coefficient was always lower than 0.7). When de distance is equal or greater than a wavelength the correlation coefficient was always lower than 0.2.

Macroscopic space diversity

In [58] a MAC technique has been tested for indoor environments with two base station transmitters (transmitting a CW at 1700 and 1701 MHz respectively) and a mobile receiver. The distance between BS was between 50 and 120 m and LOS and NLOS cases were studied. Measures were made in the worst case, when the field strength is weakest and the receiver is equidistant from the BS. Measurements show that the signals coming from the two BS were uncorrelated (correlation coefficient lower than 0.2).

Combination of macroscopic and microscopic space diversity

If MAC is combined with MIC, then the MAC only has to reduce the long fading component and in this case the gain will not decrease so rapidly when the selection intervals are made longer. If only the long fading is considered, the minimum time between change of base stations can be as long as 0.1 s without reducing the gain of the macroscopic diversity too much (with a speed of 2m/s in an indoor environment and working at 1700 MHz band).

Comparison between macroscopic and microscopic space diversity

Cell-Size	Environment	$\Delta s(\lambda)$	ρ	COST231 TD
Pico-Cell	Indoor	0.5	0.34	(90)094
	"	0.75	0.32	"
	"	2.5	0.25	(93)014
	"	2.5	0.23	(93)027
	Out&Indoor	6	0.25*	(93)008
	Indoor	7	0.12	(93)014
Micro-Cell	Outdoor	4	0.83	(95)019
	"	6.5	0.18	(92)120
	"	8	0.54	(95)019
	"	9	0.48	"
	"	10	0.12	(92)120
Small-Cell	Outdoor	10	0.34	(92)120

Table 3.2 Cross-correlation ρ, versus antenna separation Δs (* 10 MHz BW). Last column is the corresponding COST231 document number.

In [59] measurements to test the performance of macro, medium and micro space diversity have been performed, obtaining reduction in fading margin or its equivalent the diversity gain considering the total fading (long and short term). Table 3.2 shows a summary of measured micro diversity envelope cross-correlation coefficient versus antenna separation for different cell size and different propagation environments.

Polarisation diversity

As the previously mentioned techniques, the polarisation diversity is only effective in suppressing fast fading if the signals received (co-polarised and cross-polarised) are uncorrelated.

In [60] validation of polarisation diversity technique under different conditions (LOS and NLOS) by means of the evaluation of the correlation coefficient between received signals was done. In all the measurements the correlation coefficient was lower than 0.6

3.4.4 Mobile antenna diversity

[61] considers angle at the mobile unit. The antenna consists of four corner reflectors fed by monopoles and was positioned on the roof of a van. Also an omnidirectional vertical dipole was used as a reference antenna positioned above the corner reflector antenna. The experiments show that this antenna is effective in removing deeper nulls.

3.4.5 Wideband Correlation

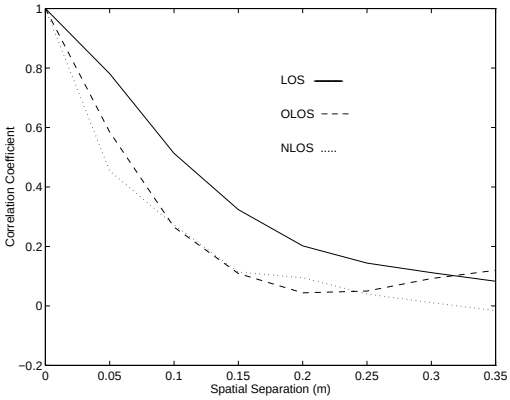

Fig. 3.20 Average autocorrelation of the instantaneous rms delay spread versus separation in indoor environments at 1800 MHz [67].

The correlation of the instantaneous rms delay spread between diversity branches gives an estimate of the ability to reduce the effects of time dispersion. It has been shown for pico-cells that a spatial separation of 2.5λ introduces uncorrelated instantaneous delay spread values between the branches [62]. In a NLOS micro-cell environment the correlation of delay spread values was estimated to 0.4 [63],[65], achieving a reduction of 20% in the delay spread selecting the smallest instantaneous value of each branch. For these experiments a novel downlink base station diversity measurement technique was employed [64],[63]. In indoor environments the diversity improvement, related to the decrease of rms delay spread, was estimated to almost 30% by means of polarisation diversity [66].

In a wideband channel the autocorrelation of the instantaneous rms delay spread gives the spatial separation necessary to achieve significant diversity improvement. This is shown in Fig 3.20 [67] after measuring in indoor LOS, OLOS and NLOS environments. It can be seen that a separation of 2λ gives uncorrelated delay spread values in all the investigated indoor scenarios. These results are in agreement with measurements using antenna diversity in a DECT system in indoor pico-cells[68].

3.5 Combining Techniques

Peter Karlsson, Telia, Sweden

Diversity combining techniques fall in two major groups

- Selection (switching, scanning, selection)
- Summation (equal gain, maximum ratio, optimum combining)

The first group is characterised by that only one branch signal yields active output at a time. Contrary the schemes in the second group apply weights to all the branch signals and the output signal is formed as a sum of all the branch signals. Each of the techniques is a trade-off between performance and complexity. The first group techniques apply to simple compact low-cost solution implementation, whereas the latter group techniques have better performance but require more hardware. There is a further distinction in the level of implementation

- Pre-detection (RF or IF implementation)
- In-detection (equalisers, soft-detection MLSE etc.)
- Post-detection (baseband implementation)

The in-detection implementation is system specific whereas both pre- and post-detection combiners can be used in general. Post-detection requires multiple receiver branches. Pre-detection provides higher gain due to coherent summation possibilities.

It is necessary to establish the combining strategy on the appropriate criteria for a given radio system. These criteria are typically

- Carrier to noise ratio C/N (narrowband systems)
- Signal to interference ratio C/I (high capacity systems)
- Irreducible BER due to ISI (digital radio system) [62], [68].

The two first criteria are aimed for maximisation in the combining process whereas the latter is aimed for minimisation.

3.5.1 Gain and complexity for different combining techniques

The switched diversity combining technique offers the lowest complexity, since only one receiver is used, while switching between antenna branches. The switch diversity is mostly a pre-detection combining technique and the switching algorithm is based on a threshold level, causing the receiver to switch from one antenna to the other if the signal is below the threshold. When wideband digital radio modems are considered, it is better to base the switching algorithm on a BER threshold or a combination of BER and RSSI. Examples of combiner performance have been made using data from wideband measurements at 1800 MHz with a terminal speed of 1 m/s in micro- and pico-cell environments [69]. Analysis of the switch combiner in a DECT type of receiver shows only a marginal improvement over a single branch [70].

When true selective combining (SC) is used, the best signal of the branches is selected. This post-detection requires one receiver pr. diversity branch. In [68] a hybrid selection/switch combining technique was presented, where the RSSI selection was based on two RF-receiver parts. However, the demodulation can be performed in a single baseband receiver after fast switching between the branches. In a digital radio system it is possible to use the preamble of each frame in order to measure or monitor the RSSI level. By means of this technique it possible to emulate the performance of selection diversity based on the RSSI level using only one [71].

Further improvement of the diversity performance can be obtained if equal-gain combining (EGC) or maximal-ratio combining (MRC) is used. By weighting the signals from the antennas according to the maximal-ratio technique, the SNR is in theory 3 dB better relative to selective combining when two independent branches are used. The combining according to SC and MRC using data measured in two

branches separated 2.5 λ, show that the diversity improvement follows the theoretical results [72].

Equal-gain combining is not so complex to implement as MRC, since the weights are omitted. A coherent equal gain combiner is then referred to as a pre-detection scheme. As a result the diversity gain is only 1 dB lower than if MRC is used, but the EGC technique is still better than selective combining in narrowband and time-invariant channels. In a wideband system like DECT, with a frequency selective and time-variant channel, the selective combiner gives better performance than EGC [70].

3.5.2 Influence of the time-variant channel

The coherence time Δt_c of the channel determines the lower limit of the combining rate. When selection or switching combining technique is used, the best branch has to be determined at a rate higher than the channel variations in order not to deteriorate the diversity performance. Accordingly, when MRC or EGC is used the rate of the weight and/or phase adjustments must be higher than the channel variations.

In the frequency domain the channel variations are given by the Doppler spread B_d, which can be approximated with the maximum Doppler shift f_d. Thus, the radio channel is highly time-variant if the surrounding environment and/or the terminal is moving fast in relation to the carrier wave-length. An example of the diversity gain versus the combining rate for different schemes is shown in Fig. 3.21. The narrowband result is based on measurements at 1700 MHz in indoor environments [73] and the wideband results are based on simulations of switch and selection combining in a DECT system presented in [71]. Note that the combining rate r_c of the wideband characteristics in this example is an approximate estimation of the rate of the DECT system. Nevertheless, in relation to the channel variations, i.e. normalised to the Doppler shift f_d, it is possible to make comparisons between different systems and combining techniques. The normalised combining rate $\upsilon_{cr} = r_c / f_d$ is then equivalent to the number of possible combining adjustments per wave-length. The comparison in Fig. 3.21 indicate that the combining rate must be at least 3 times the Doppler shift when SC is used. The rate of switching combining must be up to 10 times the Doppler shift in order to take advantage of the decorrelated diversity branches.

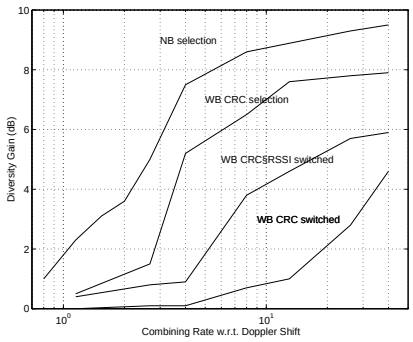

Fig. 3.21 Diversity gain for a narrowband system with RSSI selection and for a wideband system with switch or selection combining based on RSSI and/or CRC as a function of the normalised combining rate υ_{cr}.

In a system where the long-term fading is mitigated by macro diver-

sity the combining rate can be approximately one order of magnitude lower than if the short-term fading is to be reduced [73]. The spatial auto-correlation of the long-term fading component determines the necessary combining rate for different terminal speeds, in agreement with the rate for the short-term channel variations presented in Fig. 3.21.

3.6 Macro and Micro Diversity Gain

Peter Karlsson, Telia, Sweden

The probability of insufficient transmission quality over a radio channel, can be reduced by means of diversity techniques. Antenna diversity is one of the possible techniques to compensate both for the short term fading and for the long term fading and, hence, the link reliability is increased. The diversity performance is related to the decorrelation between two or more separate antennas, which are used at the mobile terminal and/or at the base stations. In the narrowband case, i.e. when frequency-flat fading is considered, the diversity gain G_D expresses the possible reduction of a given fading margin M. A wireless cellular system must have an area coverage of 99% to give the same reliability as the fixed network. Thus, the fading margin must be large enough to support the required service reliability. In many typical situations the short term fading is almost Rayleigh distributed, while the long term fading is log-normal distributed with a standard deviation σ of up to 10 dB. If antenna diversity with two uncorrelated branches is used in such a scenario, the 99% level fading margin M_{99} can be reduced by 10 dB considering the short-term fading when selection combining is used. Accordingly it possible to reduce the long-term fading margin M_{99} by 10 dB in this scenario using selection combining. In the wideband case, i.e. when the fading is frequency-selective, it is also possible to reduce the effects of time dispersion by means of antenna diversity. Here, the separation between the antennas must be large enough to be able to give decorrelated power delay profiles. Thus, the diversity performance is better when the power and the time delays of the multipaths at each antenna are different.

3.6.1 Macro Diversity

The macroscopic diversity scheme can improve the link quality by combining the signals between the mobile or portable terminal and two or more base stations. Then the effects of the long-term fading, which is mainly caused by shadowing objects, e.g. buildings and hills in macro-cells, large vehicles and trees in micro-cells and walls and furniture in pico-cells, are reduced. In this macro diversity scenario the spatial separation Δs corresponds to the cell sizes, which is equivalent to the distance between the base station sites. It is obvious that macro diversity has the strongest impact on the cell boundaries, where the local mean from at least two base stations are almost the same. Thus, at the boundaries it is possible to reduce the long-term fading

margin by an appropriate combining of signals with low correlation. For outdoor macro-cells we can assume that the envelope of the long-term fading components are uncorrelated, since the propagation paths between the mobile and the base stations are totally different. An analysis of the correlation between the long-term fading at two base stations in a microcellular environment was made in [63]. The result verifies the assumption of uncorrelated long-term fading and the average power level by selecting the best branch increases. However, the measurements show that the macro diversity gain is only significant in areas where the mean levels of the attenuation between the mobile terminal and the base stations are similar. Furthermore, in some micro-cellular environments (antennas below roof-tops) the long-term fading can be partially correlated if the same shadowing object appears in both propagation paths.

Level (dB)	No Div.	Δs=9-17λ		No Div.	Δs>=350λ	
Environment	M_{99}	M_{99}	G_D	M_{99}	M_{99}	G_D
LOS	13.8	7.5	6.3	19.6	10.4	9.2
OLOS	9.2	6.0	3.2	10.2	5.5	4.7
NLOS	9.0	7.2	1.8	11.1	8.9	2.2

Table 3.3 Fading margins and diversity gain of the long-term fading using two antenna separations in indoor environments.

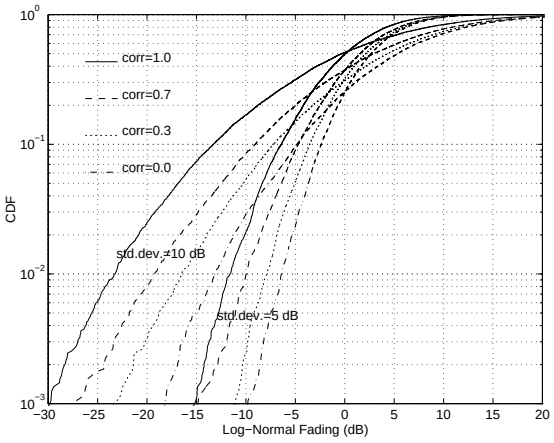

Fig. 3.22 Cumulative distribution of the log-normal long-term fading, with standard deviations 5 and 10 dB. A selection diversity scheme with the correlation coefficients 0, 0.4, 0.7 and 1 has been used.

To be able to fulfil a given area coverage reliability the long-term fading margin can be reduced relative to the variations and the spatial correlation of the radio links. In theory it is possible to reduce the long-term fading margin by 10 dB if two uncorrelated branches with selection combining are used and the standard deviation of the fading is 10 dB. Of course, the gain increases with lower correlation and larger variations. Measurements at 1700 MHz in indoor environments using simultaneously sampling of the narrowband power at two receivers have been made [73]. The receiver separation was in the range 40 m to 100 m, which corresponds to a typical base station separation. Measurements in similar environments but using the antenna separation 17 λ in LOS and OLOS and 9 λ in NLOS are also included for a comparison. The correlation is

approximately 0.3 for the larger separation and 0.7 for shorter separation. The results concerning the possible reduction of the long-term fading are shown in Table 3.3.

The simulated macro diversity gain for two branches and selection combining are given in Table 3.4, where the 99% area coverage reliability level has been used. Note that the standard deviation of the log-normal distributed long-term fading and the spatial correlation coefficients are used as parameters. These simulated results agree closely with the diversity gain estimated from measurements in indoor environments [73]. As an example, the cumulative distribution of the log-normal fading of a single branch and when selective combining between two branches is used, are shown in Fig. 3.22.

The log-normal fading has a standard deviation of 5 and 10 dB in this example and the correlation between the branches is 0, 0.4, 0.7. Note that the distribution of a single branch is equivalent to the distribution of a diversity scheme with the correlation coefficient 1.0.

Level (dB)	ρ=1.0	ρ = 0.0		ρ = 0.4		ρ = 0.7	
σ (dB)	M_{99}	M_{99}	G_D	M_{99}	G_D	M_{99}	G_D
5	11.7	9.8	4.6	10.2	3.0	12.3	1.6
8	18.6	10.2	8.5	10.7	5.4	12.2	2.8
10	23.3	13.3	10.0	6.5	6.9	6.9	4.1

Table 3.4 Macrodiversity fading margin M_{99} and gain G_D for the log-normal fading component with standard deviation 5, 8 and 10 dB for three correlation levels between two branches.

3.6.2 Micro Diversity

The short-term power fluctuations around the local mean, i.e. when the long-term fading component is removed, can be mitigated by two antennas co-located at the same mobile terminal or base station. In this case the effects of the short-term fading can be reduced if the envelopes are uncorrelated. If the scattered waves arrive at the two antennas from all directions, a horizontal separation Δs of approximately $\lambda/2$ gives a correlation coefficient of less than 0.2. This is in general the case in indoor environments and at mobile terminals in outdoor environments, where local scatterers give a uniform distribution of incoming waves. At base stations on roof tops a larger separation is necessary to combat the fading from the otherwise correlated signals [74]. Micro diversity implemented at base stations show a significant gain when two antennas are used, while it is difficult to obtain low correlation between three or more branches [25].

Level (dB)	No Div.	Δs=9-17λ		Δs=2.5 λ	
Environment	M_{99}	M_{99}	G_D	M_{99}	G_D
LOS	12.5	4.7	7.8	5.8	6.7
OLOS	16.7	7.6	9.1	8.3	8.4
NLOS	17.4	8.8	8.6	9.2	8.2

Table 3.5 Estimated fading margins and diversity gain by selection of strongest signal measured in two separate branches.

Measurements have been made at 1700 MHz in different propagation environments in order to quantify the correlation between the envelopes at two separated antennas and the corresponding diversity gain. The envelope correlation estimated from measurements of the narrowband signals at two antennas separated by 2.5λ was 0.3, 0.2 and 0.3 in LOS, OLOS and NLOS indoor environments respectively [73]. The corresponding diversity gain using selection combining was estimated to 6.5, 8.3 and 8.6 dB in these LOS, OLOS and NLOS propagation scenarios. The experimental estimation of the diversity gain was also made using the horizontal antenna separation 17 λ in LOS and OLOS, while 9 λ was used in NLOS. The correlation coefficients were estimated to 0.0, 0.1 and 0.3 respectively and the corresponding diversity gain based on selection of the sampled values are presented in Table 3.5.

To be able to achieve uncorrelated branches at short antenna separations, it is efficient to use polarisation diversity. However, the diversity gain decreases if the mean levels of the branches are different (XPD<>0dB). This is specially the case in LOS. Measurements with one co-polarised and one cross-polarised antenna have been made both in LOS and NLOS indoor environments [66]. The diversity gain, related to the 99% reliability level, by using selection between the two branches was 6.3 dB. Hence, there is no significant reduction of the diversity gain due to different mean levels.

The theoretical diversity gain reaches 10 dB with selective combining in a Rayleigh fading environment, if the branches are uncorrelated. However, the gain is lower in a Ricean fading environment, since the probability of deep fades is less than in the Rayleigh fading case. In practice all the variations will be smoothed out by means of the spatial diversity and the instantaneous SNR is improved, which reduces the BER. Simulations of the Ricean distributed short fading amplitude in two different branches have been made to evaluate the diversity gain versus correlation. The simulated diversity gain for a Ricean fading channel with K-factors in the range from 0 to 4 are presented in Table 3.6 The gain corresponds to a scheme where instantaneous selection combining is assumed, i.e. selection at each sample point is allowed. Note that the channel is Rayleigh fading when K=0, which is the worst case of the short-term fading component. The channel is almost Rayleigh fading in typical NLOS environments, and here the Ricean parameter K=0 or K=1. In OLOS environments typical average values for K is in the range 2-3, while the average K-factor in LOS environments is equal to 3 or 4.

The simulated diversity performance, considering the necessary fading margin for the 99%-level M_{99} and the corresponding diversity gain G_D, agree with the results from measurements presented above. The diversity gain is approximately 6 dB in LOS, 7 dB in OLOS and 9 dB in NLOS environments when the envelope correlation $\rho = 0.3$. This is a typical correlation level in practical antenna configurations, but the gain is still high when the branch correlation $\rho = 0.7$, see Table 3.6.

Level (dB)	ρ=1.0	ρ = 0.0		ρ = 0.3		ρ = 0.7	
K-factor	M_{99}	M_{99}	G_D	M_{99}	G_D	M_{99}	G_D
0	19.6	9.8	9.8	10.2	9.4	12.3	7.3
1	19.1	10.2	8.8	10.7	8.3	12.2	6.8
2	16.6	8.4	8.2	8.7	7.9	9.9	6.7
3	14.2	6.2	8.0	6.5	7.7	7.6	6.6
4	11.8	6.0	5.8	6.5	5.3	6.9	4.9

Table 3.6 Simulated levels of fading margins and the corresponding diversity gain versus envelope correlation for the short-term fading with five different Ricean K-factors. Note that ρ=1.0 is equivalent to the performance without diversity.

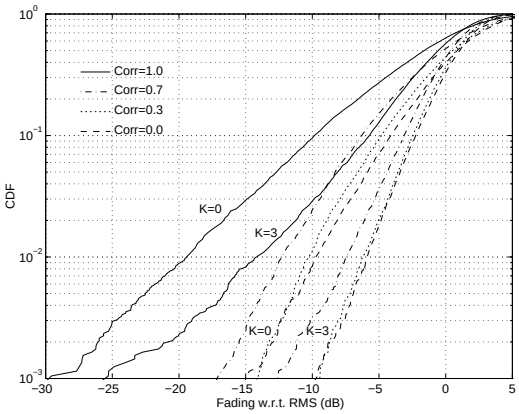

Fig. 3.23 Cumulative distribution of the short-term fading using two-branch selection diversity with the correlation coefficients 0, 0.3, 0.7 and 1. Note that $\rho_{env}=1$ is equivalent to the CDF without diversity, i.e. a single branch.

The simulated cumulative distributions of the short term fading when K=0 and K=3 are shown in Fig. 3.23. The CDF's using instantaneous selection combining between the branches with different correlation levels, are also shown. The simulated results of diversity performance agree with the experimental gain found in typical Ricean channels [73].

It is also possible to reduce the long-term fading margin with micro diversity in environments were the spatial auto-correlation of this component is "short". Hence, if the antenna separation exceeds the size of the shadowing objects, e.g. furniture, stairs and people, the diversity gain of the total fading is larger than if only short-term fading is considered [67]. In pico-cells a separation of 2-3 m between the antennas give partially decorrelated branches, i.e. ρ≅0.7, and the total diversity gain

is then given by the reduction both of the long-term and short-term fading components.

3.6.3 Wideband Diversity Performance

If the channel is frequency selective within the given system bandwidth the problem with ISI can also be reduced by means of antenna diversity. In this case the correlation of the instantaneous rms delay spread between the diversity branches gives an estimate of the possibility to reduce the effects of time dispersion. Of course, the diversity gain increases when the time dispersion in the separate branches gets more uncorrelated.

The correlation of the delay spread values of two separate branches measured in NLOS micro-cell environments was estimated to 0.4 [63]. A 20 % reduction of the delay spread was then achieved by selection of the smallest instantaneous value of each branch. The time dispersion effects can also be reduced by means of antenna polarisation diversity, which was shown in [66]. The diversity improvement, related to the decrease of rms delay spread, was estimated to almost 30 % using the data from these measurements in indoor environments [66]. The spatial diversity makes it possible to increase the coverage area of a cell for a given system quality, since the delay spread in general increases with the cell sizes. In a system like DECT the maximum delay spread for a BER of 10^{-3} can be increased from 90 ns to approximately 200 ns, when selection diversity is used [75].

3.7 References

[1] E. Zollinger, *Properties of Indoor Radio Channels (in German : Eigenschaften von Funkübertragungsstrecken in Gebäuden)*. Ph.D. ETH No. 10064, Zürich: Swiss Federal Institute of Technology Zürich, Switzerland, Nov. 1993.

[2] A. Heilman, *Antennas I* (in German : *Antennen I)*. Mannheim: Bibliographisches Institut, Hochschultaschenbücher-Verlag, 1970.

[3] H. Meinke and F. W. Gundlach, *High-Frequency Engineering Handbook (in German : Taschenbuch der Hochfrequenztechnik)*. Berlin: Springer, 4th ed., 1986.

[4] R. C. Johnson and H. Jasik, *Antenna Engineering Handbook*. New York: McGraw-Hill, 2nd ed., 1984.

[5] A. S. Duchene and J. R. A. Lakev, "The IRPA guidelines on protection against non-ionizing radiation", in *The Collected Publication of the IRPA*, chapter 5, New York: Pergamon Press, 1991, pp. 72-82.

[6] Y.J. Guo, A. Paez, R.A. Sadeghzadeh, and S.K. Barton, "A patch antenna for HIPERLAN", to appear in Wireless Personal Communications, Special Issue on HIPERLAN.

[7] Y. S. Wu and F. J. Rosenbaum, "Mode chart for microstrip ring resonators", *IEEE Trans. Microwave Theory Techn.*, vol. 21, no. 7, July 1973, pp. 487-489.

[8] R. G. Vaughan, "Two port higher mode circular microstrip antennas", *IEEE Trans. Antennas Propagat.*, vol. 36, no. 3, March 1988, pp. 309-321.

[9] L. C. Shen, S. A. Long, M. R. Allerding, and M. D. Walton, "Resonant frequency of a circular disc printed-circuit antenna", *IEEE Trans. Antennas Propagat.*, vol. 25, no. 5, July 1977, pp. 595-596.

[10] P. F. M. Smulders, *Broadband Wireless LANs: A Feasibility Study*. Ph.D., Eindhoven: Technical University Eindhoven, CIP-Data Koninklijke Bibliotheek, Den Haag.

[11] K. Uenakada and K. Yasunaga, "Horizontally polarized biconical horn antenna excited by TE_{11} mode in circular waveguide", *Trans. IECE*, vol. 54-B, Dec. 1971, pp. 125-126.

[12] W. L. Stutzman and G. A. Thiele, *Antenna Theory and Design*. New York: John Wiley & Sons, 1981.

[13] F. Schwering and A. A. Oliner, "Millimeter-Wave Antennas", *Antenna Handbook*. New York: Van Nostrand Reinhold Company Inc., 1988, pp. 7-1 to 7-150.

[14] C. A. Fernandes, P. O. Francês, and A. M. Barbosa, "A dielectric lens antenna for the MBS demonstrator", RACE 2067, *RACE Mobile Telecommun. Workshop*, Amsterdam, vol. 2, May 1994, pp. 733-740.

[15] C. A. Fernandes, P. O. Francês, and A. M. Barbosa, "Dielectric lens antenna for a mobile application at millimeterwaves", in *Proc. 17th ESA Antenna Workshop*, Noordwijk, Holland, July 1994.

[16] C. A. Fernandes, P. O. Francês, and A. M. Barbosa, "Shaped coverage of elongated cells at millimeterwaves using a dielectric lens antenna", in *Proc. 25th Europ. Microwave Conf.*, Bologna (IT), Sept. 1995, pp. 66-70.

[17] T. Tage and K. Tsunekawa, "A built-in antenna for 800 MHz portable radio units", in *Proc. Int. Symp. Antennas Propagat.*, Japan, Aug. 1985.

[18] S. Seki, N. Kammuri, and A. Sasaki, "Detachable unit service in 800 MHz band cellular radiotelephone system", *IEEE Commun. Mag.*, vol. 24, no. 2, Feb. 1986, pp. 47-52.

[19] J. Rasinger, A. L. Scholtz, W. Pichler, and E. Bonek, "A new enhanced-bandwidth internal antenna for portable communication systems", in *Proc.40th IEEE Veh. Techn. Conf.*, VTC'90, Orlando (FL), May 6-9, 1990, pp. 7-12.

[20] J. Rasinger, E. Bonek, K. Laukkanen, V. Santomaa, and A. L. Scholtz, "The important role of internal antennas in new personal communications", *ITU Technical Symposium, Integration, Interoperation and Interconnection: The Way to Global Services*, part 2, vol. II, Oct. 10-15, 1991, pp. 195-199.

[21] T. Tage and K. Tsunekawa, "Performance analysis of a built-in planar inverted-F antenna for 800 MHz band portable radio units", *IEEE J. Select. Areas Commun.*, vol. 5, no. 5, June 1987, pp. 921-929.

[22] R.H. Clarke, "A statistical Theory of Mobile-Radio Reception", *Bell Syst. Techn. J.*, 1968, pp. 957-1000.

[23] T. Aulin, "A modified model for for the fading signal at a mobile radio channel", *IEEE Trans. on Veh. Techn.*, Vol. VT-28, No. 3, 1979, pp.182-203.

[24] A.M.D. Turkmani, J.P. Parsons, "Characterisation of mobile radio signals : base station crosscorrelation", *IEE proc.*, Vol. 138, No. 6, Dec. 1991, pp. 557-565.

[25] W.C. Jakes (editor), *Microwave Mobile Communications*, IEEE Press classic reissue, USA 1993.

[26] P.C.F. Eggers, "Quantitative Descriptions of Radio Environment Spreading relevant to Adaptive Antenna Arrays", *EPMCC'95* conf. proc., Bologna Italy, 28-30 Nov. 1995, pp.68-73

[27] P.C.F. Eggers, "Angular Dispersive Mobile Radio Environments sensed by highly Directive Base Station Antennas", *IEEE PIMRC'95* conf. proc., Toronto Canada, September 1995, pp.522-526

[28] P.C.F. Eggers, G.F. Pedersen, K. Olesen, "Multi sensor propagation", RACE II *TSUNAMI deliverable R2108/AUC/WP3.1/DS/I/046/b1*, D.3.1.1, August 1994.

[29] A.J. Levy, J.-P. Rossi, J.-P. Barbot and J. Martin, “An improved sounding technique applied to wideband mobile 900 MHz propagation measurements”, *IEEE VTC’90 conf. proc.*, May 6-9 1990, Orlando FL USA, pp. 513-519.

[30] O. Nørklit, P.C.F. Eggers, J. Bach Andersen, “Jitter Diversity in Multipath Environements”, *45th IEEE VTC conf. proc.*, Chicago, USA, July 25-28 1995, pp. 853-857.

[31] R.W. Lorenz, “Comparison of the digital mobile radio systems in Europe (GSM) and in Japan (JDC) with special attention on the business aspects” (in German : “Vergleich der digitalen Mobilfunksysteme in Europa (GSM) und in Japan (JDC) unter besonderer Berücksichtigung der Wirtschaftlichkeitsaspekte”), *Der Fernmelde Ingenieur*, Verlag für Wissenschaft und Leben Georg Heidecker Gmbh Erlangen, heft 1,2 Januar/Februar 1993.

[32] J-P. deWeck, J. Ruprecht “Real-Time ML estimation of very frequency selective multipath channels”, *IEEE Global Telcom. Conf.* proc., San Diego, USA, 1990, pp.2045-2050.

[33] F. Adachi, M.T.Feeney, A.G.Willianson, J.D.Parsons, “Crosscorrelation between the envelopes of 900mhz signals received at a mobile radio base station site”, *IEE Proc., Pt. F*, Vol. 133, No. 6, Oct. 1986, pp.506-512.

[34] A.F. Molisch, J. Fuhl, and E. Bonek, “Pattern distortion of mobile radio base station antennas by antenna masts and roofs”, *Proc. 25th Europ. Microwave Conf.*, Bologna Italy, 1995, pp. 71-76.

[35] H. Hollmann, “Base Station Antennas for Sector-Shaped Service Areas in Mobile Radio Communications”, *Proc. of Int. Symp. on Antennas and EM theory*, URSI/CIE, 1985, pp. 712-717.

[36] R. Rathgeber, F.M. Landstorfer, R.W. Lorenz, “Extension of the DBP field strength prediction programme to cellular mobile radio”, *proc. of ICAP 91*, York UK, 15-18 April 1991, pp.164-167.

[37] P.E. Mogensen, S. Petersen, “Antenna configuration measurements for DECT micro cells”, *IEEE/ICCC proc. PIMRC’94/WCN*, The Hauge, 1994, pp. 1075-1080.

[38] T. Bull, M. Barret, R. Arnott, “Technology in Smart Antennas for Universal Advanced Mobile Infrastructure (TSUNAMI R2108) Overview”, *RACE Mobile Telecom. Summit* proc., Cascais Portugal, Nov. 22-24 1995, pp. 88-97.

[39] Q.Garcia, F. Muncio, “Broadband Base station Arrays and Antenna Elements for Mobile Communications”, *EPMCC’95* conf. proc., Bologna Italy, 28-30 Nov. 1995, pp.56-61

[40] J. Wigard, P.E. Mogensen, F. Fredriksen, O. Nørklit, “Evaluation of Optimum Diversity Combining in DECT”, *IEEE PIMRC’95* conf. proc., Toronto Canada, September 1995, pp.507-511

[41] TSUNAMI, “Seminar and demonstration of adaptive antennas”, *notes Center for PersonKommunikation*, Aalborg University, Denmark, 18th January 1996.

[42] O. Nørklit, “Jitter Diversity Measurements”, *COST231 TD(96) 21*, Belfort, France, 24-26 Jan. 1996.

[43] R. Passerini, M. Frullone, M. Missiroli, G. Riva, “Performance of Adaptive Antenna Arrays for Wideband Indoor Communications”, *Proc. of IEEE VTC’96*, Atlanta USA, 28 April - 1 May,1996.

[44] J. Fuhl, J-P. Rossi, E. Bonek, “Characterization of the Urban Mobile Radio Channel by 2D Direction-Of-Arrival Estimation”, *COST231 TD(96) 12*, Belfort, France, 24-26 Jan. 1996.

[45] G.F. Pedersen, J. Bach Andersen, “Integrated Antennas for Hand-held Telephones with Low Absorbtion”, *44th IEEE VTC proc.*, Stockholm Sweden, June 8-10 1994, pp. 1537-1541

[46] J. Fuhl, P. Nowak, E. Bonek, “Improved internal antenna for hand-help terminals”, Electronics Letters 30 , 1994, pp.1816-1818.
[47] N. Kuster, T. Schmid, K. Meier, “Investigations of the absorbtion in the extreme near field of transmitters” (in German : “Untersuchungen der Absorption im extremen Nahfeld von Sendern”), *ETH Zurich*, : Swiss Federal Institute of Technology Zürich, Switzerland 1993.
[48] J. Toftgård, S.N. Hornsleth, J. Bach Andersen, “Effect on Portable Antennas by the Presence of a Person.”, *IEEE Trans. Antennas and Propagation* ,vol. 41, No. 6, June 1993, pp. 739-746
[49] P.C.F. Eggers, “Envelope Correlation Coefficients of Rayleigh fading signals corrupted by additive gaussian noise”, *COST231 TD(96)02*, Belfort France 24-26 Jan. 1996. A further development is found in P.C.F. Eggers, “Diversity evaluation based on Correlation properties of Rician/Rayleigh fading signals subject to additive Gaussian noise”, proc. *IEEE PIMRC’97*, Helsinki Finland, sept. 1997, pp.1064-1068.
[50] W.C.Y.Lee “Effects of correlation between two mobile radio base station antennas” IEEE Trans.Commun. vol. COM-21, no.11, Nov. 1973, pp.1214-1224.
[51] A.M.D.Turkmani, A.A.Arowojolu, P.A.Jefford and C.J.Kellett “An experimental evaluation of the performance of two-branch space and polarization diversity schemes at 1800 Mhz”, IEEE Trans. Vehic. Techn. Vol.44, no.2, May 1995, pp. 318-326.
[52] P.E. Mogensen, F. Fredriksen, C. Verholt, CPK Aalborg University, Denmark, “Antenna diversity measurements for fixed RLL”, COST231 TD(95)019, Bern Switzerland, Jan. 1995.
[53] P.E Mogensen, S Petersen, “Antenna configuration measurements for DECT microcells”, *proc. PIMRC’94/WCN*, The Hague the Netherlands, sept. 21-23 1994, pp. 1075-1080.
[54] R.G. Vaughan, “Polarization diversity in mobile communications”, *IEEE trans. on Vech. Techn*., Vol. 39, No. 3, Aug. 1990, pp. 177-186.
[55] P.C.F. Eggers, J. Toftgård, A.M. Oprea, “Antenna Systems for Base Station Diversity in Urban Small and Micro Cells”, *IEEE J-SAC*, Vol. 11, No.7, September 1993, pp.1046-1057.
[56] P.E. Mogensen, “GSM Base-Station Antenna Diversity Using Soft Decision Combining on Up-link and Delayed-Signal Transmission on Down-link”, proc. *IEEE VTC’93*, Secaucus NJ USA, May 18-20, pp. 611-616.
[57] S. Ruiz-Boque, A. Baldovinos & R. Agusti, “Fading and Diversity Measurements Inside Buildings”, *COST231 TD(90)094*
[58] P. Karlsson, “Investigation of Radio Propagation and Macroscopic Diversity in Indoor Microcells at 1700 Mhz”, *COST231 TD(90)052*.
[59] P. Karlsson, “Body Effects and Diversity Performance in Indoor Radio Channels at 1700 Mhz”, *COST231 TD(93)014*
[60] S. Ruiz-Boque, “Polarization Diversity for Indoor Mobile Communications”, COST231 *TD(93)7*
[61] A. Koivumaki, “Direction Diversity Measurements at 900 Mhz”, *COST231 TD(91)035*
[62] G. Kadel, Simulation of the DECT system using wideband channel data measured in two diversity branches, *Proc. of 2nd ICUPC*, Ottawa, Canada, 1993.
[63] G. Kadel, Measurement of wideband micro- and macro-diversity characteristics of the mobile radio channel, *IEEE Proc. of VTC’94*, Stockholm Sweden, June 8-10 1994, pp.165-169.

[64] R.W. Lorenz, G. Kadel, “Diversity measurement technique for wideband mobile radio”, proc. GLOBECOM, Houston USA, 1993, pp. 1237-41

[65] M. Grigat, G. Kadel, “Wideband micro- and macrodiversity characteristics of the mobile radio channel,” RACE Mobile Telecom. Workshop, Amsterdam Netherlands, May 1994, pp. 688-692

[66] P.E. Mogensen, Wideband Polarization diversity measurements for wireless personal communications, *Proc. of Nordic Radio Symposium NRS’92*, Aalborg Denmark, June 1-4 1992, pp. 49-53.

[67] P. Karlsson, “Indoor Radio Propagation for Personal Communications Services”, *LUTEDX/(TETE-1011)/1-132(1995)*, Ph.D. Thesis, Lund University, Mar. 1995.

[68] P.E. Mogensen and S. Petersen, Practical Considerations of Using Antenna Diversity in DECT, *IEEE Proc. of VTC’94*, Stockholm Sweden, June 8-10 1994, pp.1532-1536.

[69] P.C.F. Eggers, J. Toftgård, “Assessment of Base Station Antenna Diversity Efficiency in Frequency Selective μ- and pico-cell Environments”, *Proc. of IEEE VTC’93*., Secaucus NJ., USA 1993, pp.572-576.

[70] P.C.F. Eggers, P.E. Mogensen, “Evaluation of Low Effort Dispersion-Reduction Techniques for DECT in Telepoint Environments”, *Proc. of IEEE VTC94*, Stockholm, Sweden, 1994, pp.677-680

[71] P.E. Mogensen et al., “Evaluation of an Advanced Receiver Concept for DECT”, *IEEE Proc. of VTC’95*, Chicago, U.S.A., July 25-28, 1995, pp. 514-519.

[72] G. Kadel and R.W. Lorenz, “Impact of the radio channel on the performance of digital mobile communications”, *IEEE Proc. of PIMRC’95*, Toronto, Canada, Sept. 27-29, 1995, pp. 419-423.

[73] P. Karlsson, “Measuring and Modelling of the Indoor Radio Channel at 1700 MHz”, LUTEDX/(TETE-7062)/1-101(1992), Lund University, Aug. 1992.

[74] W.C.Y. Lee, *Mobile Communications Design Fundamentals*, John Wiley & Sons Inc., New York, 1993.

[75] L. Lopes, “An Overview of DECT Radio Link Research in COST 231”, *IEEE Proc. of PIMRC’94*, The Hague, The Netherlands, Sept. 18-22, 1994, pp. 99-104.